Protein and Nonprotein Cysteinyl Thiol Modification by *N*-Acetyl-*p*-benzoquinone Imine via a Novel *Ipso* Adduct†

Weiqiao Chen,‡ John P. Shockcor,§ Robert Tonge,‡ Ann Hunter,‡ Carlos Gartner,‡ and Sidney D. Nelson*,‡

Department of Medicinal Chemistry, University of Washington, Seattle, Washington 98195, and Drug Metabolism & Pharmacokinetics Department, Dupont Pharmaceuticals, Newark, Delaware 19714

Received January 20, 1999; Revised Manuscript Received April 21, 1999

ABSTRACT: *N*-acetyl-*p*-benzoquinone imine (NAPQI), a reactive metabolite of acetaminophen (APAP), can arylate and oxidize protein and nonprotein thiols in the pathogenesis of APAP-induced hepatotoxicity. We report the first direct evidence for the formation of a labile *ipso* adduct between glutathione (GSH) and NAPQI using a combination of techniques including liquid chromatography/tandem mass spectrometry and liquid chromatography/NMR spectroscopy. Decomposition kinetics of the GSH−NAPQI *ipso* adduct and product ratios suggested that the *ipso* adduct was readily reversible back to NAPQI under neutral and basic conditions. The significance of the *ipso* adduct is that it may migrate from its site of formation to other cell compartments where it can either oxidize protein thiols or covalently modify them. *Ipso* adduct formation with protein thiols was demonstrated with a cysteine protease, papain, whose catalytic activity relies on the presence of an active site cysteinyl thiol. The formation and reactions of cysteinyl thiol *ipso* adducts of NAPQI provides significant new insights into possible reactions of quinone imines with cellular peptides and proteins.

Although most reactions of quinones and quinone imines with nucleophiles yield 1,4-conjugate addition products (*1*), some reactions yield 1,2 addition products such as quinone monoketals (*2*) and quinone imine ketals (*3*). These *ipso* adducts of quinones and quinone imines are relatively stable and are useful intermediates in organic synthesis where they undergo a variety of addition, substitution, and elimination reactions (*2, 3*). However, the formation of *ipso* adducts in biochemical reactions has never been directly demonstrated, and little is known about their fate.

N-acetyl-*p*-benzoquinone imine (NAPQI)[1] is a quinone imine that is formed by cytochrome P450 oxidation of acetaminophen (APAP), a widely used analgesic and antipyretic drug (*4*). NAPQI is highly reactive (*5*), and there is substantial evidence that it is responsible for initiating events that lead to hepatotoxicity in humans when large doses of APAP are taken (*6*−*8*). NAPQI is not only an electrophile that can form covalent adducts with nucleophiles such as glutathione (GSH) and protein thiols (*9, 10*), but it also is a powerful chemical oxidant with a standard reduction potential, $E° = 0.978 \pm 0.001$ V (*11*). Thus, covalent binding and oxidation of nonprotein and protein thiols by NAPQI have been implicated in the pathogenesis of hepatotoxicity caused by APAP.

Early studies of APAP metabolism showed that cellular GSH played an essential role in protecting against liver toxicity and that protein arylation by a reactive metabolite of APAP in vitro was prevented by the addition of GSH (*12*). The 3-position of the aromatic ring (C-3′) was determined by ^{1}H and ^{13}C NMR to be the site of conjugation with GSH (*13*). Cysteinyl thioether conjugates at the same position of the aromatic ring were characterized as protein-bound residues of APAP (*14*). This position has been assumed to be the only site of conjugation, although the 1, 2, and 4 positions of the aromatic ring also could be sites of conjugation based on their presumed chemical reactivity (Figure 1).

The formation of a labile *ipso* adduct (Meisenheimer-type complex) of GSH with NAPQI was suggested based on observations from different laboratories (*15*). First, although ascorbic acid rapidly reduces NAPQI back to APAP both chemically and when formed in hepatic microsomes, it has little effect in hepatocytes in vivo (*4, 16*). Second, a thioether *ipso* adduct of a dimethylated analogue of APAP has been synthesized (*17*), and its precursor quinone imine has several characteristics in common with NAPQI (*10, 18*). Third, although NAPQI chemically reacts very rapidly in the presence of excess GSH to form 3′-glutathion-*S*-yl−APAP (3′-GS−APAP), GSSG, and APAP in a 2:1:1 ratio (*19*), GSSG concentrations in livers of APAP-treated mice increase several hours after initial marked decreases in hepatic GSH and protein thiol concentrations, indicating the formation of some intermediate capable of breakdown to form GSSG (*20, 21*). Last, the formation of such an intermediate would help explain the binding of APAP to proteins in subcellular

† This work was supported by National Institutes of Health Grants GM-25418 and GM-32165 (to S.D.N.).

* To whom correspondence should be addressed. Telephone: (206)-543-1419. Fax: (206)685-9297. E-mail: sidnels@u.washington.edu.

‡ University of Washington.

§ DuPont Pharmaceuticals.

[1] Abbreviations: NAPQI, *N*-acetyl-*p*-benzoquinone imine; APAP, acetaminophen; GSH, reduced glutathione; GSSG, oxidized glutathione; AMAP, 3′-hydroxyacetanilide; LC/MS/MS, liquid chromatography/tandem mass spectrometry; LC/NMR, liquid chromatography/NMR spectroscopy; CID, collision-induced dissociation; 2′-GS−APAP, 2′-glutathion-*S*-yl−APAP; 3′-GS−APAP, 3′-glutathion-*S*-yl−APAP; DTT, dithiothreitol.

10.1021/bi990125k CCC: $18.00
Published on Web 05/28/1999

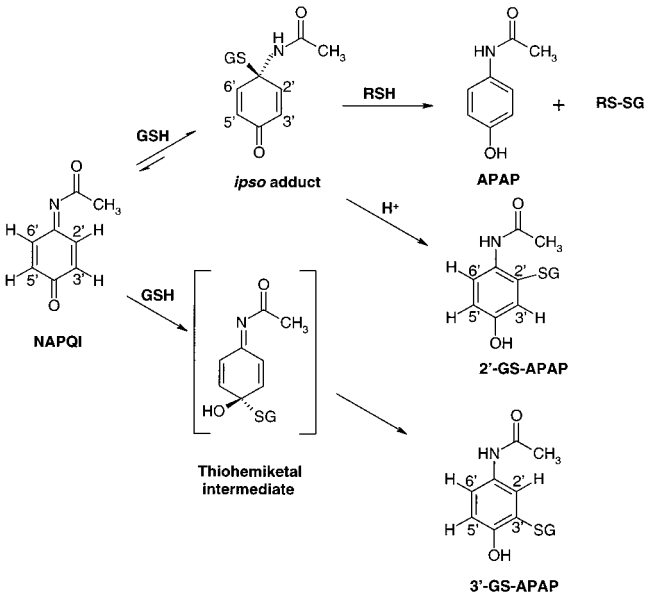

FIGURE 1: Proposed mechanisms for the formation of the three GSH conjugates of APAP. The thiohemiketal *ipso* adduct, shown in brackets, is only a postulated intermediate that has not been characterized; 3′-GS−APAP may be formed by direct 1,4-addition at C-3′.

compartments other than the endoplasmic reticulum where NAPQI is formed (*20*−*24*) and even to extracellular proteins such as hemoglobin (*25*). On the basis of the results presented in this paper, the *ipso* adduct may migrate from its site of formation to other cell compartments and serve as a latent form of NAPQI.

We propose that one or more *ipso* adducts, formed by reaction of protein and nonprotein thiols (such as GSH) with NAPQI, are quasi-stable intermediates that have sufficient stability to react with thiols (and possibly other nucleophilic groups) at sites distant from the formation of NAPQI. We report here direct physicochemical evidence for the formation of an *ipso* adduct of NAPQI with GSH using a combination of techniques including liquid chromatography/tandem mass spectrometry (LC/MS/MS) and liquid chromatography/NMR spectroscopy (LC/NMR). Reactions of the *ipso* adduct were then investigated under a variety of conditions.

Since NAPQI also may react with protein thiols to form *ipso* adducts in biological systems, the possible formation and reaction of *ipso* adducts of NAPQI with a model protein, papain, was investigated. Papain is a member of a family of cysteine proteases that have been isolated from a large number of biological sources including bacteria, plants, and animals (*26*). Papain has an active site that is relatively accessible to small molecular weight chemicals (*26*), and its catalytic activity, which relies on an active site thiolate anion, can be easily and very sensitively assayed (*27*). Therefore, papain was used to study the reaction of NAPQI with cysteinyl thiols in a protein, to provide insights into the adduct formed.

EXPERIMENTAL PROCEDURES

Synthesis. NAPQI was synthesized using previously described methods (*5*). APAP (2 g) was oxidized with 4 g of freshly prepared dry silver oxide in 100 mL of dry chloroform with sonication. The reaction was monitored by thin-layer chromatography (diethyl ether mobile phase, R_f of NAPQI is 0.63). After 30 min, the suspension was vacuum filtered through Celite into a flask containing 5 mg of butylated hydroxytoluene. The volume of solution was reduced to 10 mL on ice using an aspirator before placing the sample on a vacuum-dried silica gel column. NAPQI was eluted by flash chromatography with diethyl ether as a bright yellow band. The band was collected and reduced in volume to 2−3 mL in an ice-cooled flask using an aspirator. The final amount of ether was removed by high vacuum (0.05 mmHg) before subliming (0.01 mmHg) the NAPQI at room temperature onto a cold finger cooled in dry ice−acetone. NAPQI was recovered as bright yellow crystals, mp 73−74.5 °C (literature 74−75 °C, ref *5*) and stored at −70 °C desiccated under argon until used. All procedures were carried out in oven-dried, acid-washed glassware and, where possible, under a dry argon atmosphere.

2′-Glutathion-*S*-yl−APAP (2′-GS−APAP) and 3′-GS−APAP were synthesized and purified as follows. NAPQI was synthesized as described above except that dry acetonitrile was used instead of chloroform. Silver oxide was removed by centrifugation. To the NAPQI in acetonitrile was added an equivalent amount of GSH dissolved in water with vigorous stirring. A white precipitate formed and was removed by centrifugation. Acetonitrile was removed by rotary evaporation, and the remaining dark brown solution was added to 20 mL of 50 mM potassium phosphate buffer, pH 7.4, containing 5% acetonitrile. 2′-GS−APAP and 3′-GS−APAP were then purified by HPLC with a Beckman ODS Ultrasphere column (10 mm × 25 cm, 5 μm). The mobile phase was 5% acetonitrile and 0.05% trifluoroacetic acid in water, and the retention times for 2′-GS−APAP and 3′-GS−APAP were 21 and 33 min, respectively.

Instrumentation and Analytical Methods. Proton NMR spectra of 2′-GS−APAP and 3′-GS−APAP were recorded at 200 MHz on a Bruker AMX 200 spectrometer. The samples, which were purified by the preparative HPLC method described above, were dissolved in D_2O, and a trace amount of HOD was used as the chemical shift reference.

Mass spectrometry and LC/MS/MS were carried out on a Micromass Quattro II triple quadrupole mass spectrometer equipped with an atmospheric pressure ion source and an electrospray interface. Analyses were performed with an ionizing voltage of 3.8 kV, and nitrogen was used as the nebulizing gas. Cone voltage was set at 23 V, and collision energy was set at 19 V. Collision-induced dissociation (CID) of the precursor ion at *m*/*z* 457 was performed in the rf-only quadrupole region and employed argon as target gas at a gas pressure of 1.0×10^{-3} mbar. Separation was performed on a 3.5 μm Zorbax SB-C18 column (4.6 mm × 15 cm) with a Shimadzu LC-10AD pumping system. A SPD-1AV variable dual wavelength UV instrument was used for UV detection. 5% CH_3CN in 20 mM ammonium acetate buffer, pH 6.0, was used for the mobile phase. The flow rate was 1 mL/min, and 50 μL/min of the flow entered the mass spectrometer via a splitter. The retention times of the GSH conjugates of APAP were 2.0 min for the *ipso* adduct, 3.0 min for 2′-GS−APAP, and 3.8 min for 3′-GS−APAP based on HPLC−UV detection. The retention time on the LC/MS/MS system was delayed about 0.5 min due to dead volume in the connecting tube between the UV detector and MS ion source.

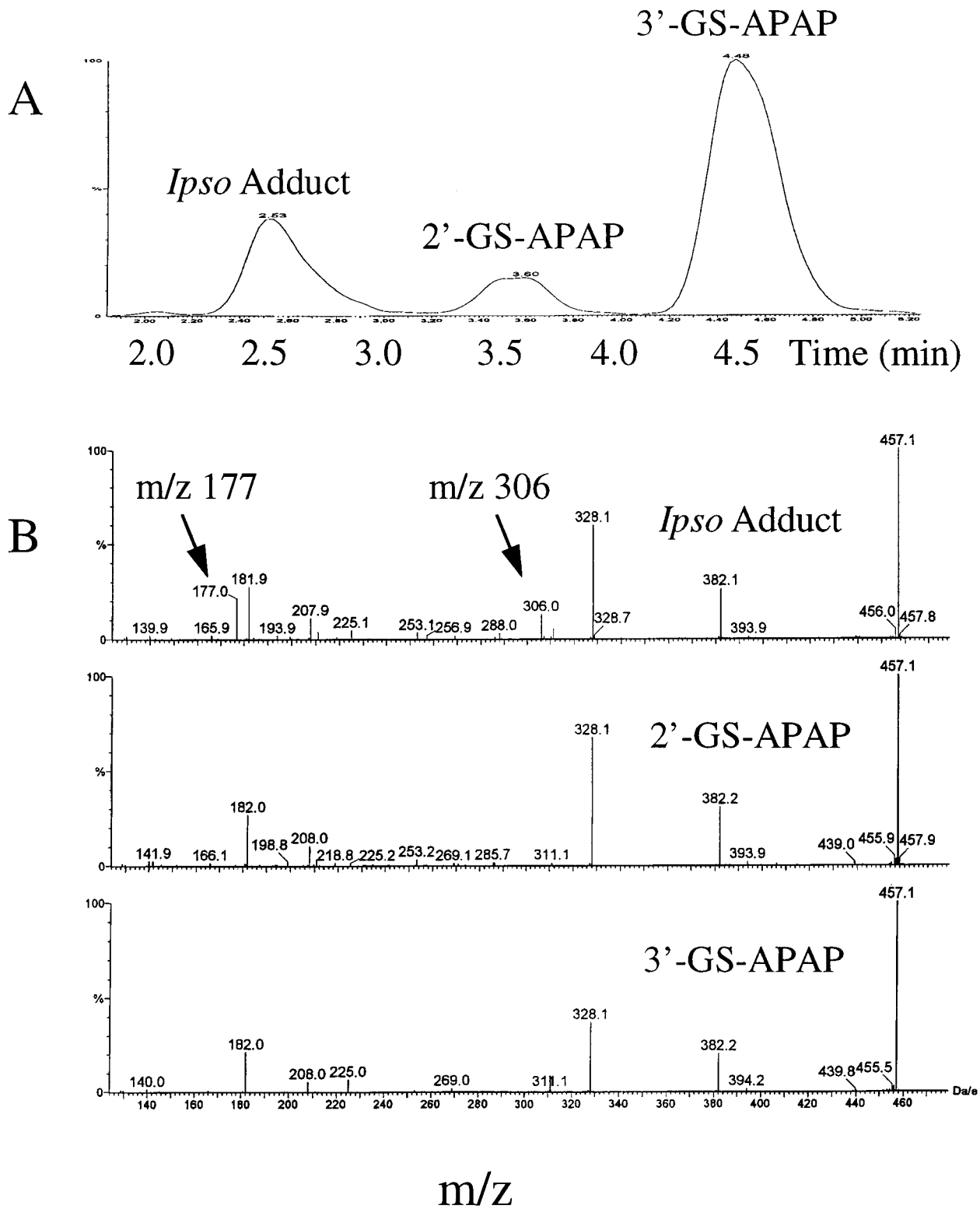

FIGURE 2: (A) LC/MS/MS chromatogram of the reaction products of equimolar concentration of NAPQI and GSH at pH 6.0 using 20 mM ammonium acetate as the mobile phase. (B) Product ions spectra obtained by collision-induced dissociation of a precursor ion at *m*/*z* 457 in the LC/MS/MS chromatogram.

GSH in water was mixed with equimolar NAPQI dissolved in CH_3CN at room temperature. The reaction mixture was immediately injected onto the LC/MS/MS system for analysis. Three peaks with an identical mass-to-charge ratio at *m*/*z* 457 ($M + H^+$ of a GSH conjugate of APAP) were observed (Figure 2). The first peak (approximately 1 mL) was collected into a microcentrifuge tube containing 100 μL of 10 mM cysteine, and the volume was reduced by lyophilizing. The remaining sample was then analyzed by LC/MS/MS.

The LC conditions used for LC/NMR were identical to those used in the LC/MS/MS experiments except that deuterium oxide (D_2O) was used in place of water. A Bruker LC22 pump delivered the mobile phase. The eluent from the column was monitored at 254 nm using a Bischoff Lambda 1010 UV detector. ^1H NMR spectra were obtained

in stop-flow mode using a Bruker Avance 500 NMR spectrometer equipped with a $^{1}H/^{13}C$ LC/NMR flow probe with a cell volume of 120 μL. Suppression of the residual water and acetonitrile signals was carried out using the WET solvent suppression method (*28*). Data were acquired with 256 transients in 16K data points with a pulse repetition time of 2.8 s. Chemical shifts were referenced to acetonitrile at δ 2.0 ppm.

Decomposition of the Ipso Adduct. The stability and decomposition kinetics of the *ipso* adduct were examined under acidic, neutral, and basic conditions. The *ipso* adduct was isolated by HPLC using the conditions already described, and 100 μL of 1 M potassium phosphate buffer at pH 5.0, 6.0, 7.0, and 8.0 were added to the collected sample (1 mL) that was in 20 mM ammonium acetate buffer, pH 6.0, containing 5% CH_3CN. Addition of 0.5% (v/v) glacial acetic acid into 20 mM ammonium acetate buffer, pH 6.0, brought down the pH to 4.0. Samples were added into a quartz cuvette, and the decomposition was followed on a Beckman UV−Vis spectrophotometer. The absorption at 255 nm for the *ipso* adduct was greater than the absorption at this wavelength for the aromatic products, 2′-GS−APAP, 3′-GS−APAP, and APAP. Therefore, the absorption at 255 nm was monitored over time up to 60 min after which no change could be observed. The half-life of the *ipso* adduct at different pH values was calculated based on the decomposition kinetics. The products of decomposition were analyzed on a Hewlett-Packard 1090 II/L system with the UV detector set at 254 nm.

Papain Inactivation by NAPQI. Papain activity assays were carried out as described by others (*27*). A slurry of papain (50 μL) immobilized on a beaded agarose matrix (Calbiochem, LaJolla, CA) containing approximately 2 nmol of enzyme was added to 2 mL of 50 mM Tris/HCl (pH 7.5) containing 2 mM EDTA and 1% (v/v) DMSO in a 4.5-mL fluorescence cuvette. A stir bar was placed in the cuvette, and the enzyme was equilibrated at 37 °C with stirring for 5 min inside a SLM Aminco series 2 luminescence spectrophotometer (SLM Instruments, Rochester, NY). The assay was started by addition of the substrate *N*-benzoyl-L-arginine-7-amido-4-methyl coumarin hydrochloride (Bz-L-Arg-MCA) (Sigma, St. Louis, MO) to a final concentration of 0.05 mM. The activity of the papain was determined by the change in fluorescence at 440 nm with time (excitation wavelength 280 nm, 8 nm band-pass, 1 nm step, 670 V). Once the rate of reaction was linear, 85 nmol of NAPQI was added (freshly dissolved in 10 μL acetonitrile). While the catalytic activity was continuously monitored, 850 nmol of ascorbate in 10 μL of water, 850 nmol of GSH in 10 μL of water, and 1700 nmol of dithiothreitol (DTT) in 20 μL of water were added in a sequential manner at 2-min intervals.

To assess whether APAP or GS−APAP was released from papain in the above reaction procedure, a small (350 μL bed volume) column was prepared in a Pasteur pipet. The column was equilibrated with 10 column volumes of 50 mM Tris/HCl buffer, pH 7.5, containing 2 mM EDTA and 1% DMSO before adding 0.85 μmol of NAPQI in 100 μL of acetonitrile. This was washed into the column with 100 μL of Tris buffer and incubated for 30 s. The reaction was then quenched by the addition of 8.5 μmol of ascorbate in 100 μL of buffer, and the column was washed with 2.5 mL of buffer. GSH (8.5 μmol) in 100 μL of buffer was then added to the column and washed onto the column with 100 μL of buffer. This was incubated for 30 s before washing the column with 2.5 mL of buffer. Finally, 17 μmol of DTT in 200 μL was added to the column and was washed through the column with 2.5 mL of buffer. Throughout, 0.5-mL fractions were collected and assayed for APAP and 3′-GS−APAP by an electrochemical HPLC method as described previously (*29*).

RESULTS

Identification of Novel Glutathione Adducts of APAP. When NAPQI was reacted with equimolar amounts of GSH, three peaks with identical mass-to-charge ratios at *m*/*z* 457 ($M + H^+$ of a GSH conjugate of APAP) were detected by LC/MS/MS (Figure 2A). The third peak coeluted with synthetic 3′-GS−APAP. This conjugate has previously been characterized by proton NMR (*13*), and the spectrum obtained of our sample was essentially the same. In particular, the aromatic resonance signals constitute an ABX pattern with the C-5′ hydrogen at 6.9 ppm appearing as a doublet coupled to the ortho C-6′ hydrogen ($J = 8.7$ Hz) and to the meta C-2′ hydrogen ($J = 2.7$ Hz) and with the C-2′ hydrogen at 7.5 ppm appearing as a doublet coupled to the meta C-6′ hydrogen ($J = 2.7$ Hz).

The compound in the second peak from the HPLC chromatogram was obtained in milligram amounts by preparative HPLC. Its structure is proposed to be 2′-glutathion-*S*-yl−APAP (2′-GS−APAP) based on a comparison of its proton NMR spectrum with that of 3′-GS−APAP. The spectrum also showed aromatic resonance signals of an ABX spin system with little change in the chemical shifts of the hydrogens at C-5′ and C-6′ (6.8 and 7.2 ppm, respectively). As would be expected, their splitting patterns are different than those in 3′-GS−APAP since the hydrogen at C-5′ now appears as a doublet of doublets coupled to the ortho C-6′ hydrogen ($J = 8.7$ Hz) and to the meta C-3′ hydrogen ($J = 2.5$ Hz) and since the C-6′ hydrogen appears as a doublet coupled to the ortho C-5′ hydrogen ($J = 8.7$ Hz). A new resonance signal appears at 7.0 ppm for the C-3′ hydrogen that appears as a doublet coupled to the meta C-5′ hydrogen ($J = 2.5$ Hz). The resonance signal for the C-2′ hydrogen is no longer observed as it is the site of GSH conjugation. As in the structure of APAP itself, the chemical shifts of protons ortho to the phenolic hydroxy group in the GSH conjugates appear upfield of those ortho to the amide group, presumably due to the deshielding effect of the *N*-acetyl group.

The first peak in the chromatogram showed two unique product ions at *m*/*z* 306 and 177 in the CID spectrum (Figure 2B). These product ions were not observed in the mass spectra of either 2′-GS−APAP or 3′-GS−APAP. The ion at *m*/*z* 306 is suggestive of a GS^+ cation, which could possibly be formed by an *ipso* adduct structure due to a rearomatization driving force (Figure 3). The ion at *m*/*z* 177 is a characteristic neutral loss of mass 129 from the GS^+ cation (*m*/*z* 306).

Additional structural information of the compound eluting in the first peak was then obtained by LC/NMR. NMR data clearly indicated that the structure of the compound eluting in the first peak was an *ipso* adduct. The two doublets at 6.25 and 7.05 ppm have a coupling constant of 8.7 Hz and integrate for two protons. This is consistent with the AA′XX′

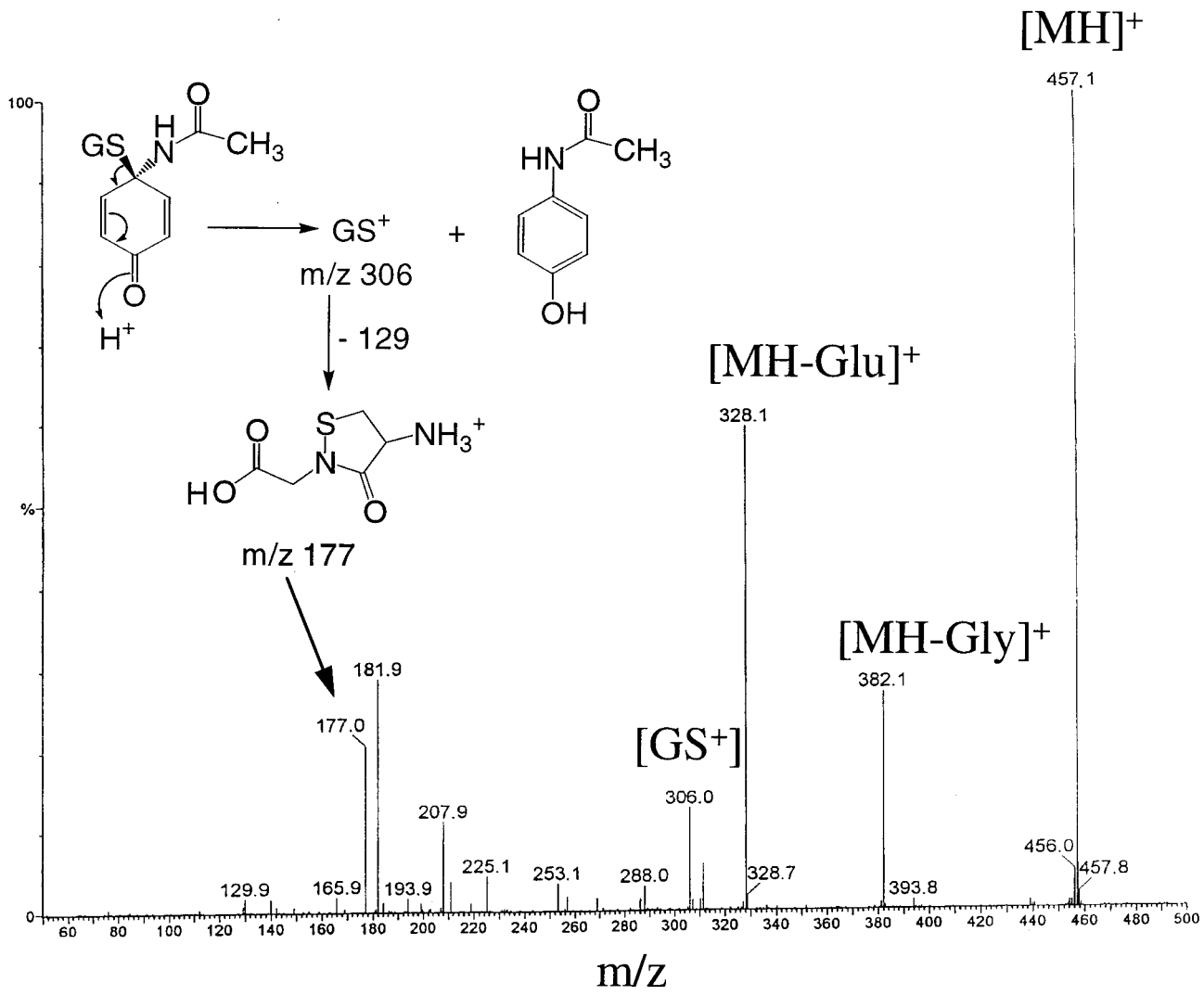

FIGURE 3: Mechanisms for the formation of fragment ions at *m/z* 306 and 177 from an *ipso* adduct of NAPQI and GSH.

spin system of the *ipso* adduct (Figure 4). The aromatic protons of the 2′- and 3′-GS−APAP show, in contrast, typical ABX spin systems consistent with a 1,2,4-trisubstituted aromatic ring. Furthermore, the marked upfield shift of the 3′ and 5′ protons are a result of vinyl conjugation in the *ipso* adduct as compared to the benzenoid aromaticity in the 2′- and 3′-adducts. The 2′ and 6′ protons are not shifted as much presumably because of deshielding by the *N*-acetyl group. Finally, the cysteinyl β-protons are shifted upfield in the *ipso* adduct because they are not affected by paramagnetic deshielding with the absence of the aromatic ring. These effects have been observed in the NMR spectra of other *ipso* adducts (*3*, *17*).

Decomposition of the Ipso Adduct. Ipso adduct decomposition was monitored by a decrease in UV absorption at 255 nm. At pH 4.0, the *ipso* adduct rapidly decomposed with a half-life of 0.5 min (Figure 5), whereas at pH 6.0 the half-life increased to 33 min. As pH increased above pH 6, the half-life again decreased.

The decomposition products were monitored by HPLC with a UV detector. The formation of 2′-GS−APAP increased as pH decreased, while the formation of both 3′-GS−APAP and APAP increased as pH increased (Table 1). At pH 4.0, 2′-GS−APAP accounted for 78% of the decomposition products, whereas 2′-GS−APAP only accounted for 15% of the decomposition products at pH 8.0. On the other hand, 3′-GS−APAP increased to 30% of the total decomposition products at pH 8.0 from 12% at pH 4.0.

Reactivity of the Ipso Adduct. No change in the concentration of the *ipso* adduct was observed in the presence of the antioxidant (reductant) ascorbic acid, but in the presence of the thiol reductant, DTT, the *ipso* adduct was converted exclusively to APAP. The reaction products of the *ipso* adduct with cysteine were examined by LC/MS. It was found that major products were the mixed disulfide of cysteine and GSH, and the reduced product, APAP, whereas only trace amounts of 3′-Cys−APAP were formed (data not shown).

Ipso Adduct Formation with Papain. The possibility of *ipso* adduct formation in a protein was investigated with the cysteine protease, papain, whose catalytic activity relies on the presence of an active site cysteinyl thiol. NAPQI was found to markedly inhibit papain activity (Figure 6). The inhibition was unaffected by sequential addition of ascorbate followed by GSH, but after the addition of DTT, the activity was completely restored. Addition of acetonitrile, ascorbate, GSH, or DTT alone did not affect enzyme activity.

A small column of immobilized papain was prepared to determine products released from the NAPQI−papain *ipso* adduct. After papain was reacted with NAPQI and excess NAPQI removed by reduction with ascorbate, subsequent

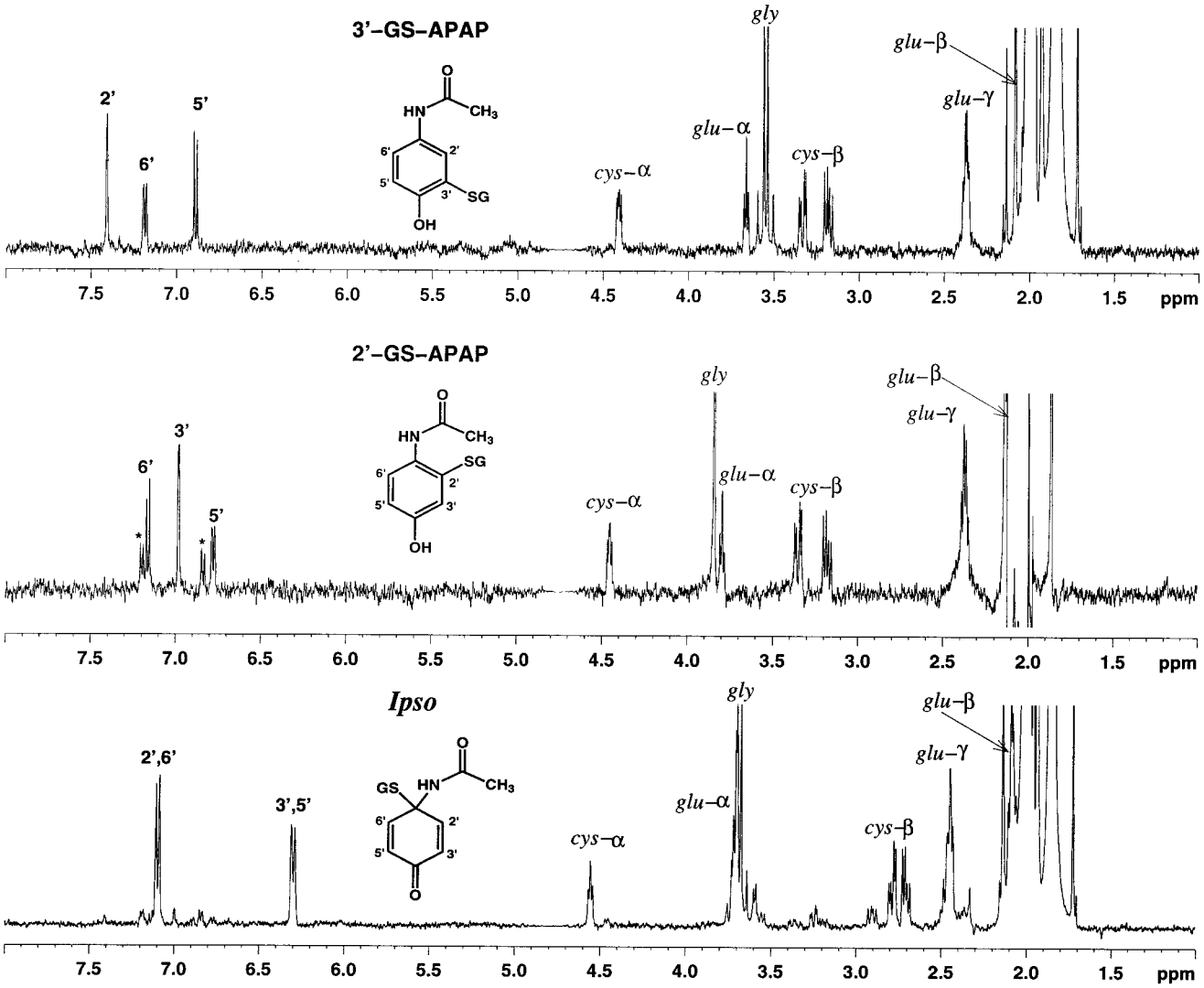

FIGURE 4: Spectra of the three GSH conjugates obtained by LC/NMR as described in Experimental Procedures. The middle spectrum for 2′-GS−APAP contains some additional resonance peaks in the aromatic region (denoted by an asterisk, *) that are from APAP itself, which coelutes under the conditions used for the HPLC separation.

addition of excess GSH resulted almost exclusively in the elution of APAP from the column with only a trace (<0.3%) of 3′-GS−APAP detected.

DISCUSSION

The nucleophilic reaction of GSH with NAPQI has primarily been viewed as a 1,4-conjugate addition reaction (Michael-type addition reaction) followed by aromatization to form 3′-GS−APAP. However, two new GSH conjugates were detected by LC/MS when NAPQI was reacted with GSH. These two novel compounds were identified as an *ipso* adduct and 2′-GS−APAP using a combination of techniques including LC/MS/MS and LC/NMR (Figures 2 and 4). Presumably, the *ipso* adduct was formed by nucleophilic addition of GSH to the imine double bond, based on the previous characterization of an *ipso* adduct of 2,6-dimethyl-NAPQI (*17*). Additional evidence that the addition occurred at the imine carbon is that decomposition of the *ipso* adduct primarily yielded 2′-GS−APAP under acidic conditions (Table 1).

Intramolecular rearrangement by a 1,2-shift of the glutathionyl moiety of an *N*-acyl-thiohemiaminal *ipso* adduct would be favored under acidic conditions (Figure 1), a reaction that has been observed with the addition of other sulfur nucleophiles to *N*-acylated imines (*30*). Under more basic conditions, both base-catalyzed elimination of GSH to reform NAPQI and nucleophilic attack of the thiolate anion of GSH to form APAP and GSSG would be favored (Figure 1). This appears to be the case, based on a decrease in the amounts of 2′-GS−APAP formed as basicity increases, with concomitant increases in the formation of 3′-GS−APAP and APAP (Table 1). We assume that 3′-GS−APAP is not formed directly from the *N*-acyl-thiohemiaminal *ipso* adduct since direct reaction of this *ipso* adduct with either excess GSH or cysteine produced only small amounts of the 3′-adduct, the major reaction being the formation of APAP and the corresponding disulfide.

An analysis of the pH rate profiles for the decomposition of the *ipso* adduct (Figure 5) also is consistent with the view that 2′-GS−APAP formation is an acid-catalyzed intramolecular reaction, whereas 3′-GS−APAP is primarily formed in a reaction that involves a separate intermediate or intermediates. At pH 4, the half-life of the *ipso* adduct is short (0.5 min), and the decomposition rate curve shows a

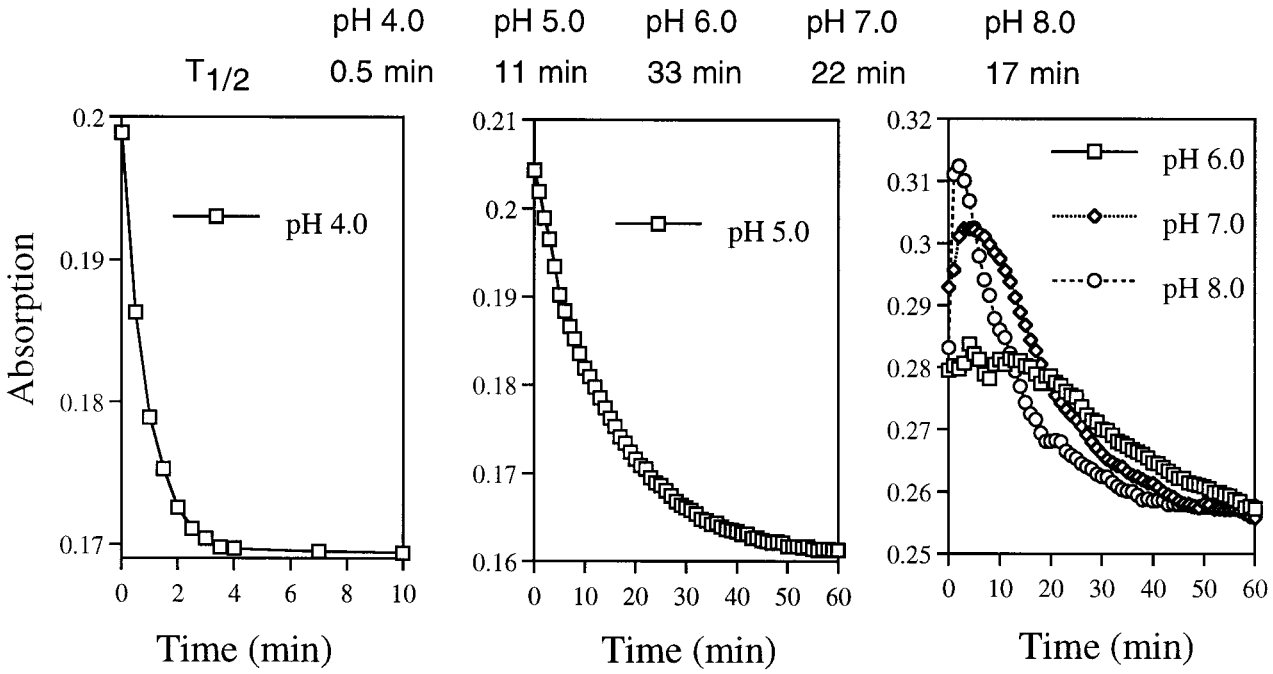

FIGURE 5: *Ipso* adduct decomposition rate profiles at different pH values. The change in UV absorption at 255 nm for the *ipso* adduct was monitored as described in Experimental Procedures. The half-life ($T_{1/2}$) of the *ipso* adduct at different pH values was calculated based on the decomposition kinetics.

Table 1: Percentages of Products Formed from *Ipso* Adduct Decomposition as a Function of pH

pH	2′-GS−APAP (%)	3′-GS−APAP (%)	APAP (%)
4.0	78	12	10
5.0	65	21	14
6.0	35	21	44
7.0	19	28	53
8.0	15	30	55

steady decline. At pH 5, the half-life is considerably longer (~11 min), and a small delay in the rate of decomposition was observed. At higher pH values the rate of decomposition was slower, and at pH 7.0 and 8.0 the absorption actually increased prior to decreasing (Figure 5). We attribute this increase to the buildup of NAPQI, which also absorbs at 255 nm in aqueous media, with a peak absorption at 266 nm (*10*). The kinetics of the reactions are complicated by the formation and hydrolysis of a carbinolamide *ipso* adduct of NAPQI at pH ≤ 6.0 (*10*, *11*) and by the reduction of NAPQI to APAP at higher pH values (*5*, *11*).

Although the mechanism or mechanisms of formation of 3′-GS−APAP, the major GSH adduct of APAP that is detectable at physiological pH, is unknown, the results of this study suggest that it is formed by rapid intramolecular rearrangement of a C-4′ thiohemiketal *ipso* adduct (Figure 1). This mechanism is consistent with thiolate addition via a "charge-controlled" reaction dictated by the high positive net atomic charge (+0.30) at C-4′ of NAPQI, with a somewhat lower positive net atomic charge (+0.18) at C-1′ (*31*), the position of attack to form the *ipso* adduct characterized herein.

How NAPQI interacts with proteins is another unanswered question. Results of our studies with papain (Figure 6) strongly suggest that an *ipso* adduct, formed by reaction of NAPQI with the active site cysteinyl thiol of this enzyme, inactivates it. Although ascorbic acid rapidly reduced excess

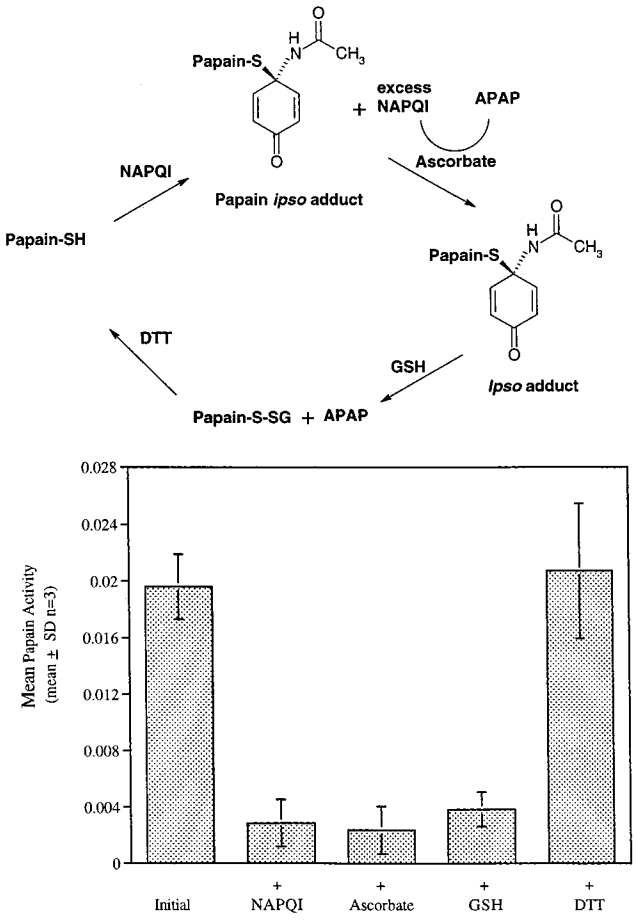

FIGURE 6: Papain inactivation and reactivation after sequential (2 min) additions of NAPQI, ascorbate, reduced glutathione (GSH), and dithiothreitol (DTT). Papain activity was measured by the change in fluorescence at 440 nm with time as described in Experimental Procedures. Note: The addition of ascorbate after the addition of NAPQI does not affect the papain *ipso* adduct but does reduce excess NAPQI to APAP.

NAPQI to APAP, it had no effect on either the activity of papain modified by NAPQI or on the synthetic glutathionyl *ipso* adduct characterized herein. These results are consistent with previously published observations that NAPQI formed chemically or by cytochrome P450 is rapidly reduced by ascorbate to APAP (*4*), but that NAPQI generated in more complex matrixes in cells reacts quickly with peptides and proteins to form adducts that are not reduced by ascorbate (*16*).

Interestingly, the addition of GSH to papain inactivated by NAPQI did not reactivate the enzyme but did release APAP from it. Presumably, GSH reacted with an enzyme-bound *ipso* adduct to form the reduced product, APAP, and generated an oxidized mixed disulfide of GSH and the protein cysteinyl thiol (Figure 6). Subsequent reduction of the *S*-thiolated protein with DTT completely reactivated the enzyme. These results are consistent with the effects of DTT on restoring protein thiols in livers of mice treated with hepatotoxic doses of APAP (*21*). Under these conditions only a small fraction (∼1/15) of the protein thiols are covalently modified irreversibly by reactive metabolites of APAP. The remainder could be either in the form of *ipso* adducts or be *S*-thiolated. Additional work is required to conclusively demonstrate *ipso* adduct formation in APAP-modified hepatic proteins, though indirect evidence exists for two of these targets (*32*, *33*).

The formation of *ipso* adducts of NAPQI provides a possible explanation for reaction of NAPQI at sites distant from its formation. The *ipso* adduct that was characterized appears to act as a latent form of NAPQI (Figures 1 and 5), i.e., it reversibly forms NAPQI in the physiological pH range. Thus, proteins and other macromolecules in the cytosol, mitochondria, cell nuclei, and cell membrane may form adducts with NAPQI originally formed from APAP in the endoplasmic reticulum. We have previously shown that mitochondria are a hepatocellular target for APAP reactive metabolites that can lead to mitochondrial Ca^{2+} dysregulation (*9*, *20*). In part, close contacts between the endoplasmic reticulum and mitochondria in cells (*34*) may be responsible for targeting this organelle by APAP reactive metabolites. However, we believe that *ipso* adducts of NAPQI also play a role, inasmuch as depletion of GSH in the mitochondria and protein adduct formation precedes GSSG formation by several hours (*20*) suggesting that an *ipso* adduct of NAPQI may be formed in the initial phase of GSH depletion; then, as GSH is resynthesized, it reacts with the *ipso* adducts to form GSSG and mixed disulfides with protein thiols, which may in turn be reduced to form GSSG.

In summary, an *ipso* adduct of NAPQI has been identified and characterized by LC/MS/MS, LC/NMR, and UV spectroscopy. The *ipso* adduct forms reversibly and may deliver NAPQI from its site of formation in the smooth endoplasmic reticulum to other subcellular compartments to cause damage. Finally, the formation and reactions of *ipso* adducts of NAPQI with proteins may provide additional insights into reactions of quinones and quinone imines with proteins and into mechanisms of APAP hepatotoxicity.

REFERENCES

1. Finley, K. T. (1974) in *The Chemistry of the Quinoid Compounds* (Patai, S., Ed.) pp 887−1144, Wiley, New York.
2. Koelsch, P. M., and Tanis, S. P. (1980) *Kodak Lab. Chem. Bull. 52*, 1−7.
3. Swenton, J. S., Bonke, B. R., Chen, C.-P., and Chou, C.-T. (1989) *J. Org. Chem. 54*, 51−58.
4. Dahlin, D. C., Miwa, G. T., Lu, A. Y. H., and Nelson, S. D. (1984) *Proc. Natl. Acad. Sci. U.S.A. 81*, 1327−1331.
5. Dahlin, D. C., and Nelson, S. D. (1982) *J. Med. Chem. 25*, 885−886.
6. Hinson, J. A. (1980) *Rev. Biochem. Toxicol. 12*, 103−130.
7. Nelson, S. D. (1990) *Semin. Liver Disease 10*, 267−278.
8. Prescott, L. F. (1996) *Paracetamol (Acetaminophen): A Critical Bibliographic Review*, pp 285−351, Taylor & Francis Ltd, London.
9. Moore, M., Thor, G., Moore, G., Nelson, S., Moldeus, P., and Orrenius, S. (1985) *J. Biol. Chem. 260*, 13035−13040.
10. Novak, M., Pelecanou, M., and Zemis, J. N. (1986) *J. Med. Chem. 29*, 1424−1429.
11. Novak, M., Pelecanou, M., and Pollack, L. (1986) *J. Am. Chem. Soc. 108*, 112−120.
12. Potter, W. Z., Davis, D. C., Mitchell, J. R., Jollow, D. J., Gillette, J. R., and Brodie, B. B. (1973) *J. Pharmacol. Exp. Ther. 187*, 203−210.
13. Hinson, J. A., Monks, T. J., Hong, M., Highet, R. J., and Pohl, L. R. (1982) *Drug Metab. Dispos. 10*, 47−50.
14. Hoffmann, K., Streeter, A. J., Axworthy, D. B., and Baillie, T. A. (1985) *Mol. Pharmacol. 27*, 566−573.
15. Smith, C. V., and Mitchell, J. R. (1985) *Biochem. Biophys. Res. Comm. 133*, 329−336.
16. Miller, M. G., and Jollow, D. J. (1984) *Drug Metab. Dispos. 12*, 271−279.
17. Fernando, C. R., Calder, I. C., and Ham, K. N. (1980) *J. Med. Chem. 23*, 1153−1158.
18. Nicotera, P., Hinds, T. R., Nelson, S. D., and Vincenzi, F. F. (1990) *Arch. Biochem. Biophys. 283*, 200−205.
19. Coles, B., Wilson, I., Wardman, P., Hinson, J. A., Nelson, S. D., and Ketterer, B. (1988) *Arch. Biochem. Biophys. 264*, 253−260.
20. Tirmenstein, M. A., and Nelson, S. D. (1989) *J. Biol. Chem. 264*, 9814−9819.
21. Tirmenstein, M. A., and Nelson, S. D. (1990) *J. Biol. Chem. 265*, 3059−3065.
22. Cohen, S. D., and Khairallah, E. A. (1997) *Drug Metab. Rev. 29*, 59−97.
23. Pumford, N. R., and Halmes, N. C. (1997) *Annu. Rev. Pharmacol. Toxicol. 37*, 91−117.
24. Qui, Y., Bennett, L. Z., and Burlingame, A. L. (1998) *J. Biol. Chem. 273*, 17940−17953.
25. Axworthy, D. B., Hoffmann, K., Streeter, A. J., Calleman, C. J., Pascoe, G. A., and Baillie, T. A. (1988) *Chem. Biol. Interact. 68*, 99−116.
26. Turk, B., Turk, V., and Turk, D. (1997) *Biol. Chem. 378*, 141−150.
27. Kanaoka, Y., Takahashi, T., Nakayama, H., Takada, K., Kimura, T., and Sakakibara, S. (1977) *Chem. Pharm. Bull. 25*, 3126−3128.
28. Smallcombe, S. H., Patt, S. L., and Keifer, P. (1995) *J. Magn. Reson. A 117*, 295−303.
29. Chen, W., Koenigs, L. L., Thompson, S. J., Peter, R. M., Rettie, A. E., Trager, W. F., and Nelson, S. D. (1998) *Chem. Res. Toxicol. 11*, 295−301.
30. Clark, W. M., and Swenton, J. S. (1990) *J. Org. Chem. 55*, 3969−3971.
31. Loew, G. H., and Goldblum, A. (1985) *Mol. Pharmacol. 27*, 375−386.
32. Gupta, S., Rogers, L. K., Taylor, S. K., and Smith, C. V. (1997) *Toxicol. Appl. Pharmacol. 146*, 317−327.
33. Dietz, E., Schafer, A., Omichimski, J. G., and Nelson, S. D. (1997) *Chem. Res. Toxicol. 10*, 1097−1103.
34. Rizzuto, R., Pinton, P., Carrington, W., Fay, F. S., Fogarty, K. E., Lifshitz, L. M., Tuft, R. A., and Pozzan, T. (1998) *Science 280*, 1763−1766.

BI990125K